



## Review article

## Continuous flow synthesis and applications of carbon dots: a mini-review

Carlotta Campalani<sup>a,\*</sup>, Davide Rigo<sup>b,1,\*</sup><sup>a</sup> Department of Molecular Sciences and Nanosystems, Ca' Foscari University of Venice, 30175 Venezia Mestre, Italy<sup>b</sup> Department of Bioproducts and Biosystems, Aalto University, Vuorimiehentie 1, Espoo 02150, Finland

## ARTICLE INFO

## Keywords:

Carbon dots  
Continuous flow  
Photocatalysis  
Microfluidics  
Hydrothermal  
Nanomaterials

## ABSTRACT

Carbon dots (CDs) are gaining growing interest within the scientific community thanks to their unique properties in high value applications. Currently, major issues are their scale-up synthesis, and the control of the reaction conditions both for their production and their application. Continuous flow (CF) chemistry and technologies can be valuable solutions to overcome these problems allowing precise control over critical synthetic parameters in a reproducible and more productive way. CF synthesis can lead to nanoparticles with more easily tunable and controllable properties (i.e. narrower size distribution and higher quantum yield) compared to common batch methodologies. In addition, the small environmental impact and high efficiency of CF can pave the way to large scale production and application of the carbon nanomaterials. For instance, supercritical water is a promising reaction medium to carry out the CF synthesis of CDs in very short time. This review showcases CF procedures for the preparation of CDs, their applications in CF photocatalysis and other niche uses, and gives some ideas on future perspectives in the field.

## Introduction

Flow systems, referred to plug flow or continuous flow (CF), offer a powerful alternative to batch reactors to carry out a variety of reactions. They give the opportunity to improve the reaction efficiency by enhancing mass and heat transfers and the overall control of the reaction parameters [1]. Particularly, CF technologies have evolved to become crucial for process intensification by substantially decreasing equipment size/production capacity ratio, energy consumption, or waste generation, and ultimately resulting in cheaper and sustainable methods [2]. Generally, the dimensions of flow reactors range from sub-millimetric (microfluidic reactors) to sub-centimetric (mesofluidic reactors) [3,4]. These configurations improve the reaction rates since reagents can be easily pressurized and heated above their normal boiling point (superheating); even more generally, thanks to a quick variation of reaction conditions (T, p, flow rate, molar ratio, concentration, etc.), rapid process optimization and scale-up can be achieved. In addition, in the case of catalytic processes, the product(s) isolation is facilitated since the catalyst is usually immobilized inside the reactor where, if necessary, it can be reactivated and reused. Another unique aspect of flow systems is the possibility to carry out multistep syntheses by designing a set-up comprised of several concatenated flow reactors. This last subject has been exhaustively reviewed elsewhere [5]. The small size of microreactors (less than 1 mm

in at least one dimension) offers additional multiple advantages in minimizing the reagent consumption and energy waste, and in improving safety during handling of hazardous chemicals and/or the conduction of exothermic reactions [6]. Moreover, a virtually instantaneous mixing can be achieved in micro-structured devices [7].

Carbon dots (CDs) are spherical carbon nanoparticles with a diameter lower than 10 nm composed by a carbogenic core and a surface rich of organic functional groups (hydroxyls, carbonyls, carboxyls...), molecular fluorophores and defects (see Fig. 1). They are mainly composed by carbon, hydrogen and oxygen and their ratio depends both on the carbon precursor and on the adopted synthetic method. In order to obtain CDs with different properties, doping elements, such as nitrogen, sulfur and others, can be introduced during the synthesis. The most used doping atom is nitrogen which generally increases the quantum yield of the CDs (QY = number of emitted photons on number of absorbed photons %) [8–10]. Concerning the morphology of the carbogenic core, it has been demonstrated that CDs can have a graphitic or amorphous nucleus depending on synthetic method and reaction conditions [11]. For instance, when using a hydrothermal treatment, amorphous materials are obtained, while pyrolysis leads to more graphitic nuclei [11].

CDs are attracting more and more interest among the scientific community thanks to their unique properties such as high biocompatibility and biodegradability, luminescence, ease of preparation and tunability, photostability, low costs, low toxicity, and high sustainability [12,13]. For

\* Corresponding authors.

E-mail addresses: [carlotta.campalani@unive.it](mailto:carlotta.campalani@unive.it) (C. Campalani), [davide.rigo@aalto.fi](mailto:davide.rigo@aalto.fi) (D. Rigo).<sup>1</sup> These authors contributed equally to the work.

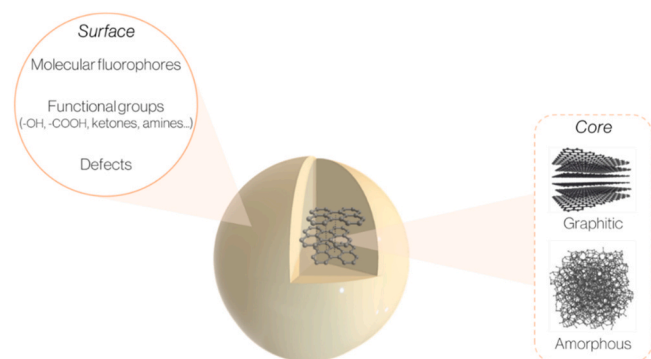


Fig. 1. Pictorial representation of the structure of CDs.

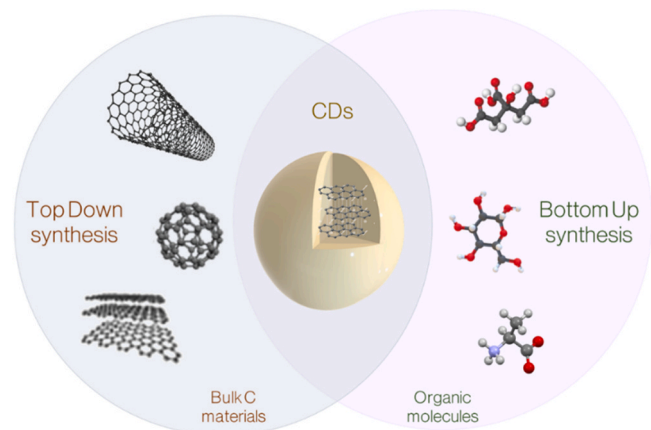


Fig. 2. Schematic illustration of the two families of synthetic methods for the preparation of CDs.

those reasons the use of CDs is spreading in a wide range of applications, from biomedical [14,15] to energy-related fields [16–20]. In addition, their great potential as light harvester and their ability to act both as electron donors and acceptors, allowed their use as photocatalysts, too [11,21–23]. Different techniques have been developed to synthesize CDs starting from a variety of carbon precursors. These synthetic pathways can be divided in two main families, namely the Top-Down and the Bottom-Up approaches. Top-Down methods involve the breakage of large carbogenic structures (graphite, graphite layers, carbon nanotubes and so on), while in the Bottom-Up the carbon nanoparticles are obtained by carbonization of small organic molecules (see Fig. 2). Among the Top-Down methods, arc-discharge, laser ablation and electrochemical oxidation can be named; these techniques allow to obtain CDs with high purity and yields and an extreme ease of size manipulation. However, Bottom-Up synthetic pathways are still the most widespread due to their simplicity and to the possibility to use a wide array of precursors. With these methods, the initial carbon precursor undergoes dehydration or decarboxylation at high temperatures ( $> 140\text{ }^{\circ}\text{C}$ ), generating the aromatic network of CDs. Among the Bottom-Up synthesis, acid oxidation, microwave treatment, and thermal-hydro/solvothermal methods can be found. The solvothermal and hydrothermal approaches involve the carbonization of the carbon precursors dissolved in an organic solvent or in water. In this case temperatures cannot exceed a certain threshold ( $140\text{--}200\text{ }^{\circ}\text{C}$ ) due to the pressure restrictions of the apparatus.

In this context, the combination of CF technologies and Bottom-Up approaches (especially hydro-/solvo-thermal) represents a timely solution for the scale-up synthesis of CDs and the control on their size and properties. CF protocols permit the control over critical synthetic variables (e.g. temperature and mass transfer) that are difficult to manage with classical methods. The possibility to have a strict control over reaction parameters like temperature, flow rates and pressure, indeed, leads to obtain CDs with more reproducible and homogeneous

characteristics. Hence, having same optical, chemical, and electronic behavior is a matter of great importance for the application of carbonaceous nanomaterials. Currently, it is still an open challenge. In addition, CF processes are less energy and time demanding, resulting in improved efficiency/productivity and a reduced environmental impact for a potential large-scale production. Together with their CF preparation, the use of CDs as photocatalysts in CF reactions is an under-explored field with a bright forecast for future development. Even though CDs have been mainly employed in CF photocatalysis, *in-continuous* bioimaging and energy storage/production are two examples of other appealing uses of CDs. Our expertise in the engineering of continuous flow procedures [24–26] and in the preparation of CDs [11,21–23] prompted us to conceptualize this mini-review, which showcases the reported works on the CF synthesis of CDs and the use of CDs in different CF reactions and *in-continuous* applications. A first section is dedicated to the synthetic methodologies, while the second part is devoted to their applications. In conclusion, highlights on the future trends and perspectives are given.

## CF synthesis of CDs

### General

In the past years, CF chemistry has been recognized as one of the potential solutions to overcome the limitations of classical batch synthesis. It is of great interest also in the field of nanomaterials hoping to reach the synthesis of tailored products in a more controllable, reproducible and productive way [27]. Nowadays, metal, metal oxides, polymers and carbon nanoparticles have been prepared by exploiting microfluidic reactors, highlighting the strong interest of the scientific community in this direction [28,29]. Despite the great potential of CF synthesis of CDs, the first report on the topic is dated in 2014 [30], and currently a handful of papers is present in the literature. The use of microreactors allows to reduce reaction times (few minutes are usually required [31]), leading to fast and extensive screenings of different conditions and involving a variety of carbon precursors, solvents and additives. In addition, a higher control on the average size of the dots can be reached by controlling the flow rate and the length, size and shape of the reactor [30]. In particular, short residence times have been related to small particles [32], while reduced reactor diameters led to a narrow distributions of CDs size due to more homogeneous and fast heat transfer [33,34]. Moreover, microreactors are less energy demanding, they minimize waste production, and facilitate handling harsh temperature and pressure conditions [35]. The use of microreactors was proved effective in increasing the QY of CDs, too [27]. Table 1 summarizes the reaction conditions of CF synthesis of CDs commented in this review with relative size, quantum yields (QY), emission wavelength ( $\lambda_{em}$ ), and application.

### CF synthesis of CDs with high QY

As mentioned, the utilization of CF reactors allowed to produce CDs with high QY. Cheng and co-workers continuously produced bright blue, fluorescent nitrogen and sulfur-doped CDs with a QY up to 68.2%. The dots, obtained from L-cysteine and citric acid, resulted to have nearly spherical shape with a mean diameter around 2.8 nm. They were prepared by continuously delivering the precursors solution into a coiled microreactor at  $180\text{ }^{\circ}\text{C}$  with a residence time of 10 min. Such CDs were demonstrated suitable for  $\text{Cd}^{2+}$  detection with high sensitivity (detection limit = 0.079 ppb) and excellent selectivity (Table 1, entry 2) [31]. CDs from citric acid and ethylenediamine were obtained with the use of three different microreactors: linear, double-snake and snake-like. The best conditions ( $T = 160\text{ }^{\circ}\text{C}$ , flow = 16 mL/min and linear microreactor) yielded carbon nanoparticles with QY of 60.1% that were applied for  $\text{Fe}^{3+}$  detection (Table 1, entry 3) [32]. A microreactor with porous copper fibers ( $T = 210\text{ }^{\circ}\text{C}$ , flow = 20 mL/min) was

**Table 1**  
CF synthesis of CDs with relative characterization and application of the works reported in this review.

Entry	Precursors	Solvent	Conditions Flow rate/residence time Temperature pressure	Reactor	Size (nm)	QY (%)	$\lambda_{em}$ (nm)	Application	Ref.
1	Different carbon sources + different nitrogen dopants	Screening of different solvents	2–10 min 180–200–220 °C Atmospheric pressure	Teflon capillary tubing (I.D. = 1 mm)	1.5–20	9–37	330–550	N.A	[30].
2	L-cysteine, citric acid	water	4 mL/min 180 °C 45 bar	Coil microreactor	2.8	68.2	425	Detection of Cd <sup>2+</sup> ions	[31]
3	Citric acid, Ethylenediamine	water	16–160 mL/min 160 °C < 5 min	Linear-like, double-snake-like and snake-like microreactor	1.8–3.0	60.1	455	Fe <sup>3+</sup> detection	[32]
4	Citric acid, different N sources	water	Atmospheric pressure 10 $\mu$ L/min 190 °C	Low Temperature Co-fired Ceramic micro-reactor	2.2–4.3	Up to 0.77	450	Metal detection and bioimaging contrast agents	[33]
5	Ascorbic acid	DMSO	17 bar 10 $\mu$ L/min 190 °C	Layered microreactor	3.3 $\pm$ 0.3	2.6	420	pH detection	[34]
6	Citric acid, Ethylenediamine	water	<i>p</i> : n.a. 20 mL/min 210 °C < 6 min	Microreactor with porous copper fibers	2.8 $\pm$ 0.2	73	460	Hg <sup>2+</sup> detection	[36]
7	Citric acid, Ethylenediamine	Water	Atmospheric pressure 190 °C < 8 min	Microreactor with foamy copper	2.47–3.34	84.1	502–521	Hg <sup>2+</sup> detection	[37]
8	Glucose, <i>p</i> -sulfonic acid, calix [4]arene	ScH <sub>2</sub> O	Atmospheric pressure 20 mL/min for water 5 mL/min for glucose 5 mL/min <i>p</i> -sulfonic acid calix[4]arene 450 °C	High pressure scH <sub>2</sub> O	1.7 $\pm$ 0.7	0.25	433	Oil recovery	[38]
9	Citric acid, ammonia	ScH <sub>2</sub> O	248 bar 20 mL/min for water 10 mL/min for citric acid and ammonia 450 °C	High pressure scH <sub>2</sub> O	3.3 $\pm$ 0.7	14.91	441	Cr <sup>6+</sup> detection	[39]
10	Glucose	ScH <sub>2</sub> O	248 bar 20 mL/min for water 5 mL/min for glucose 5 mL/min for DI water 450 °C	High pressure scH <sub>2</sub> O	2.3 $\pm$ 0.5	0.3	446	Cr <sup>6+</sup> and Fe <sup>2+</sup> detection	[40]
11	Graphene oxide, Calix[4]arene tetraphosphonic acid, KOH	ScH <sub>2</sub> O	248 bar 20 mL/min for water 5 mL/min for GO, calix[4]arene tetraphosphonic acid, KOH 450 °C	High pressure scH <sub>2</sub> O	2.26–5.38	4.5	420–510	N.A	[41].
12	Graphene oxide, <i>p</i> -tetrasulfonic acid calix[4]arene, KOH	ScH <sub>2</sub> O	248 bar 20 mL/min for water 5 mL/min for GO, <i>p</i> -tetrasulfonic acid calix[4]arene, KOH 450 °C	High pressure scH <sub>2</sub> O	1.8–3.1	2.47–3.43	440–520	N.A	[42].

(continued on next page)

Table 1 (continued)

Entry	Precursors	Solvent	Conditions Flow rate/residence time Temperature pressure	Reactor	Size (nm)	QY (%)	$\lambda_{em}$ (nm)	Application	Ref.
13	Glucose, ammonia	scH <sub>2</sub> O	20 mL/min for water 5 mL/min for glucose 5 mL/min for ammonia 450 °C 248 bar 20 min 250 °C Atmospheric pressure 2–3 s 550 °C	High pressure scH <sub>2</sub> O	4.6 ± 0.87	9.6	400–500	Cu <sup>6+</sup> detection	[43]
14	Citric acid, Urea	Water	Atmospheric pressure 20 min 250 °C	Microreactor (I.D. = 1 mm)	2.88	N.A.	From 465 to 610	Fe <sup>3+</sup> detection and bioimaging	[44]
15	EDTA, NaOH	water	Atmospheric pressure 2–3 s 550 °C	Chemical aerosol flow	< 10	22.7	400	Cellular imaging	[45]
16	Citric acid, Ethylenediamine	Tetraethylene glycol, water	Atmospheric pressure 3 mL/min 160 °C	Stainless steel coiled microreactor (I.D. = 1 mm)	10	26.95	450	Total phenol content detection	[46]
17	Ethanolamine, phosphoric acid	water	Atmospheric pressure 0.14–0.21–0.42 mL/min 110–170 °C	Stainless steel capillary microreactor (I.D. = 2 mm)	2.60	N.A.	445	N.A.	[47]
18	Milk or soy milk or orange juice or watermelon juice	water	Atmospheric pressure 30 min 120–180 °C Atmospheric pressure	Stainless steel capillary microreactor (I.D. = 2 mm)	2.17 (milk)	12.53	452	Cell imaging	[48]

N.A. = Non-Available.

developed to produce nitrogen doped CDs with high stability and QY (73 %). This study demonstrated how the porosity of copper fibers influences the elemental contents and surface functional groups of the dots: as the porosity of copper fibers decreases (from 98 % to 80 %), the QY reduced nearly two-fold (Table 1, entry 6) [36]. The same effect over reactor porosity was highlighted also in the study conducted from Tang et al., where highly fluorescent CDs with QY up to 84%; were prepared using a foamy copper flow reactor (Fig. 3) with porosities from 50 % to 98 % at 190 °C with a residence time < 8 min (Table 1, entry 7). It was demonstrated how higher porosities are related to smaller CDs with higher QY, while with lower porosities larger dots with a narrower size distribution and lower QY were noticed. This effect has been ascribed to different heat transfers and increased permanence time [37].

#### CF synthesis of CDs using supercritical water

A variety of works reported the use of supercritical water (scH<sub>2</sub>O) as a valid solvent for the continuous preparation of CDs. The H<sub>2</sub>O critical temperature (T<sub>c</sub>) and pressure (p<sub>c</sub>) are 373 °C and 220 bar, respectively. The density and dielectric constant of scH<sub>2</sub>O can be easily controlled by adjusting T and p allowing greater flexibility compared to conventional solvents. This results in the preparation of a large array of nanoparticles with tunable properties. In addition, short residence times (*i.e.* less than 2 min from injection to collection) are usually requested with scH<sub>2</sub>O as reaction medium, allowing to increase the productivity of carbon nanoparticles. In this approach, scH<sub>2</sub>O is being injected in the reactor in a counter-current manner at high temperature and pressure (above T<sub>c</sub> and p<sub>c</sub>) together with an aqueous precursor(s) solution. An example of such synthetic apparatus is shown in Fig. 4. With this method different types of CDs were obtained within short residence times (total permanence time in the system, from injection to collection, lower than 2 min). For example, Baragau and co-workers used scH<sub>2</sub>O (450 °C and 248 bar) to produce sulfur doped CDs from glucose and *p*-sulfonic acid calix[4]arene (Table 1, entry 8) [38], nitrogen-doped CDs from citric acid and ammonia (see Fig. 4 and Table 1, entry 9) [39], and non-doped CDs from glucose (Table 1, entry 10) [40]. The same approach was used also to synthesize CDs from graphene oxide *via* hydrothermal fragmentation. For example, the works by Kellici et al., reported the preparation of carbon nanoparticles starting from graphene oxide, calix[4]arene tetraphosphonic acid (or *p*-tetrasulfonic acid calix[4]arene) and potassium hydroxide using scH<sub>2</sub>O as the reaction medium (Table 1, entry 11 and 12) [41,42]. Life-cycle assessment studies established that the adopted CF hydrothermal synthesis method offers a simplified synthetic process that improves efficiency and reduces the environmental impact of the material production. In addition, it emphasizes the potential for scale-up for the continuous production of large quantities of CDs. The main difference observed in the above-reported procedures are found in the choice of the carbon precursors that led to a set of CDs with different properties. When using citric acid and ammonia (see Fig. 4) the resulting dots had an average size of 3.3 nm (from HR-TEM and AFM measurements) and demonstrated an excitation independent emission with a maximum around 441 nm due to the diversity in functional groups covering the surface of the CDs (Table 1, entry 8). X-Ray Photoelectron Spectroscopy (XPS) and FT-IR analyses confirmed the presence of C=C, C–N, C=O and O–C=O bonds together with pyrrolic/amino N–H, protonated pyridinic N, and graphitic-N on the dots surface [39]. Glucose has been also used with and without the addition of ammonia as N-doping agent [40,43]. The use of bare glucose as the carbon source for the production of CDs in scH<sub>2</sub>O led to the formation of nanoparticles with an average diameter of 2.3 nm while the doped counterpart was observed to have bigger size (4.6 nm) (Table 1, entries 10 and 13). The surface of the glucose-based CDs showed classical C=C, C=O, C–C, O–CO–C and C–OH groups, while with the addition of ammonia also pyridinic N, N–H and amide C–N were observed. Sulfur-doped CDs were also prepared using glucose, *p*-

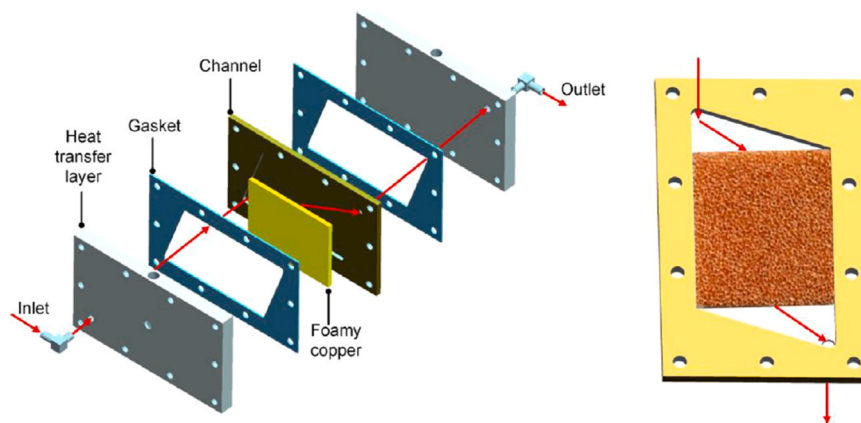


Fig. 3. Foamy copper flow reactor for the CF synthesis of CDs designed by Tang et al. Reprinted with permission from Ref. [37].

sulfonic acid and calix-4-arene. The macrocyclic molecule was described to act not only as a stabilizer and size controller, but also to affect the optical properties of the CDs [38]. Indeed, the resulting dots showed a small size with a mean diameter of only 1.7 nm (from TEM). On the surface, the presence of a plethora of oxygen containing groups was highlighted (C-C, C-O, O-C=O, carbonyls, carboxyls and hydroxyls) to whom the excellent water solubility of the dots was ascribed. The emission of the S-doped dots resulted to be excitation independent

and to have a maximum around 433 nm (Table 1, entry 8) with a good pH stability in the range 3–11. The use of calix[4]arene in the production of CDs in scH<sub>2</sub>O was exploited also using graphene oxide (GO) as the carbon precursor. In particular, the group of Kellici used GO, calix[4]arene tetraphosphonic acid/calix[4]arene tetrasulfonic acid to obtain phosphor and sulfur doped CDs, respectively (Table 1, entries 11 and 12) [41,42]. Concerning the S-doped CDs, calix[4]arene tetrasulfonic acid resulted to act as an efficient particle control agent during

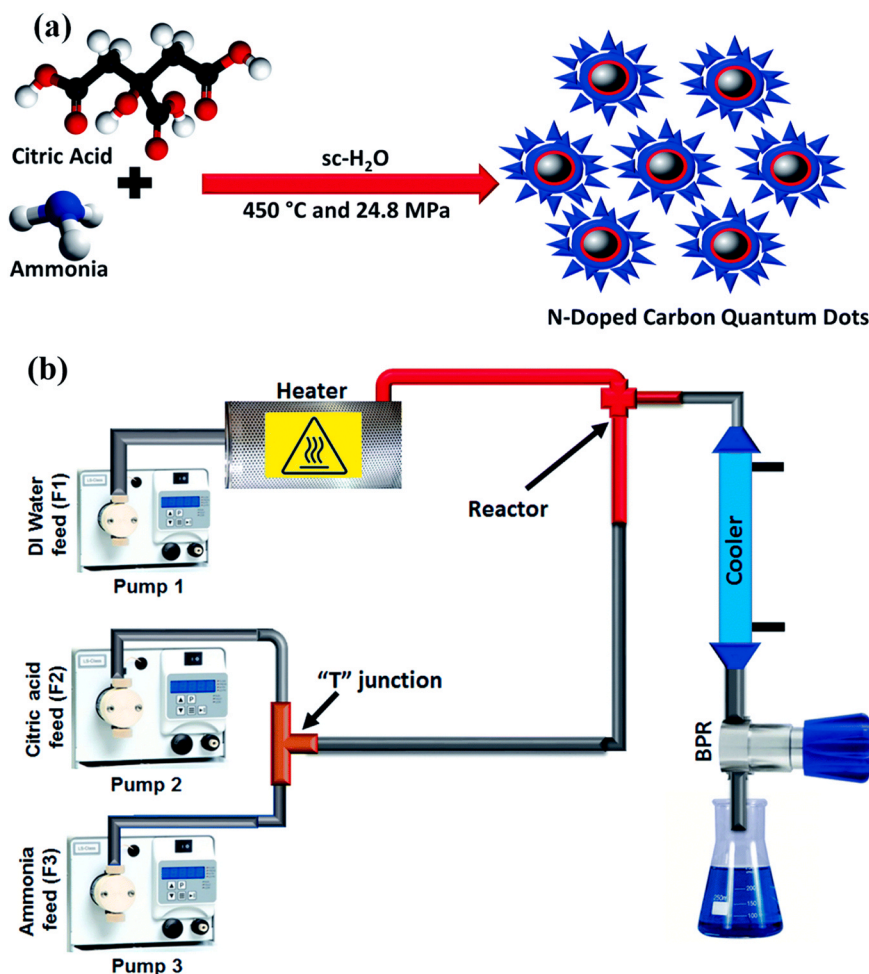


Fig. 4. Synthesis of N-doped CDs using Continuous Hydrothermal Flow Synthesis (CHFS) process with scH<sub>2</sub>O: (a) illustration of the CHFS synthesis process using citric acid as carbon source and ammonia as N-dopant, (b) simplified CHFS setup. Reprinted with permission from Ref. [39].



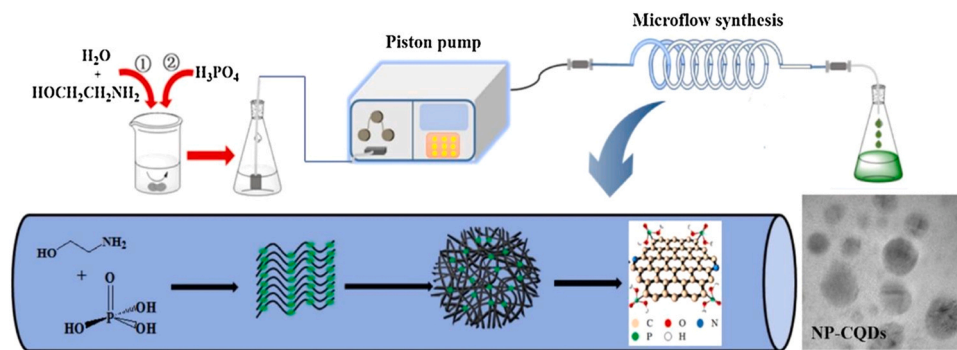


Fig. 5. Schematic illustration of the microflow synthesis of the NP-CQDs and the mechanism. Reprinted with permission from Ref. [47].

the GO fragmentation process leading to a decrease in nanoparticle size (4.3 nm without calixarene, 1.8–3.1 nm with calixarene). On the other hand, when using calix[4]arene tetraphosphonic acid the average diameter of the CDs showed a slight increase probably due to the formation of calixarene bilayers around the nanoparticles. However, in both cases, an excitation-independent emission was observed upon addition of the calixarene assigned to their narrow particle size distribution.

#### CF synthesis of CDs in water under subcritical conditions

Water under subcritical conditions (most used range:  $T = 110\text{--}250\text{ }^{\circ}\text{C}$ ,  $p = 1\text{--}45\text{ bar}$ ) remains the most common solvent for the CF preparation of carbon nanoparticles thanks to its intrinsic safety compared to  $\text{scH}_2\text{O}$  and the major setup simplicity. Berenguel-Alonso et al., developed a fully integrated low temperature ( $190\text{ }^{\circ}\text{C}$ , 17 bar) cofired ceramic micro reactor for the synthesis of CDs starting from citric acid and different nitrogen dopants (Table 1, entry 4) [33]. The as obtained pool of dots (particle size 2.2–4.3 nm) exhibited blue photoluminescence (maximum emission peak at 450 nm), QY up to 0.77 %, and they were applied for metal detection and as bioimaging contrast agents. An aqueous citric acid and urea solution was used as carbon source also from Shao and co-workers. Thanks to the use of a micro-reactor ( $T = 250\text{ }^{\circ}\text{C}$ ), they managed to reduce the conventional reaction time (12–24 h) to 20 min. The obtained dots resulted to have narrow size distribution with an average of 2.88 nm and were applied in  $\text{Fe}^{3+}$  detection (Table 1, entry 14) [44]. Nitrogen-doped CDs were continuously prepared also starting from aqueous solutions of ethylenediaminetetraacetic acid (EDTA) using a chemical aerosol flow process at  $550\text{ }^{\circ}\text{C}$  (Table 1, entry 15). This strategy resulted to be ultrafast (retention time of the droplets in the tube furnace of only 2–3 s), to have the advantage of easy separation and purification and possibility of facile scale-up. *In vitro* and *in vivo* biotoxicity tests demonstrated that the CDs produced with this method were highly biocompatible and, thus, they have great potential for cellular imaging applications [45]. Another type of nitrogen-doped CDs was obtained from citric acid and ethylenediamine using a mixed-solvent system of tetraethylene glycol and water at  $160\text{ }^{\circ}\text{C}$  and atmospheric pressure, and used for the total phenol detection in honeysuckle extracts (Table 1, entry 16) [46]. Lin et al. demonstrated also the possibility to use a stainless-steel capillary microreactor with an internal diameter of 2 mm for the continuous production of CDs ( $T = 110\text{--}170\text{ }^{\circ}\text{C}$ ) from classical carbon precursors, such as ethanolamine and phosphoric acid (Fig. 5, Table 1, entry 17) [47], and from unconventional carbon sources namely milk, soy milk, orange juice or watermelon juice ( $T = 120\text{--}180\text{ }^{\circ}\text{C}$ ) (Table 1, entry 18) [48].

#### Comparison of reported methods and general conclusions

Drawing some general conclusions on the influence of the CF reaction parameters on the structure and properties of CDs is not straightforward due to the wide variety of conditions reported (temperature, reactor type,

residence time, nature and concentration of the carbon precursors, among others). Nevertheless, some key trends can be hypothesized/extrapolated. Generally, small particle size, narrow size distribution and high quantum yield are targeted during the CDs synthesis. In addition, considering the long reaction time (12–24 h) usually required for the synthesis of CDs with conventional batch methods, another goal is to decrease the time and the energy consumption while increasing the productivity.

The clearest trends can be illustrated thanks to the work by Lu et al., who performed a screening of conditions obtaining more than 300 different types of CDs with the same microreactor [30]. In particular, in their work, type and concentration of precursors, solvents, additives, temperature and time were changed. It was observed, however, that the variations of temperature, residence time and concentration of the precursors have insignificant effects on the photoluminescence properties of the corresponding CDs. The influence of the residence time on several properties of glucose derived CDs has also been studied. Three types of CDs were prepared pumping a solution of glucose in formamide into a Teflon capillary at  $180\text{ }^{\circ}\text{C}$  for 1, 2 or 5 min [30]. The three obtained CDs showed very similar photoluminescence properties (see Fig. 6), FT-IR and XPS spectra independent on the carbonization time.

The elemental analysis of the materials proved that all the three CDs contained carbon, oxygen, hydrogen and nitrogen, but the nitrogen content increased with extension of time showing a more active participation of formamide in the carbonization process of glucose. In addition, a more evident dehydration took place at longer reaction times, reflecting in a decrease in hydrogen and oxygen, with a parallel increase in carbon. Some differences were highlighted also in the UV-Vis spectra of the CDs (Fig. 7, left). An overall major absorption was achieved from the CDs obtained in 5 min, underlining that longer reaction time generates higher extents of carbonization of the precursor and the corresponding CDs might have a larger graphitic moiety. Moreover, longer reaction time led to bigger CDs as can be seen from the TEM micrographs in Fig. 7 [30]. A similar trend was found by Shao et al., who showed that short reaction time led to smaller particle size of the dots [44].

Thanks to the reported data, it is possible to state that the variation in the residence time can help in the production of CDs with tailorable dimensions and absorptions, but does not influence directly the photoluminescence properties and the surface groups of the materials. Obviously, by using different carbon precursors and temperatures the characteristics of the products will be different. The use of higher temperature, for example, leads to an increase in the carbonization degree but it has been demonstrated that it does not influence the nature of the functional groups, the amount of doping or the fluorescence lifetime [49]. In addition, a couple of works clearly shown that porous reactors can tune the properties of the obtained dots: a decrease of the reactor porosity leads to higher QY [36,37]. This finding was related to an improved heat transfer with lower porosity which brings to a more carbonized product.

Overall, the CF synthesis of CDs allows a facile control on the properties of the dots and a safer and easily scalable production.

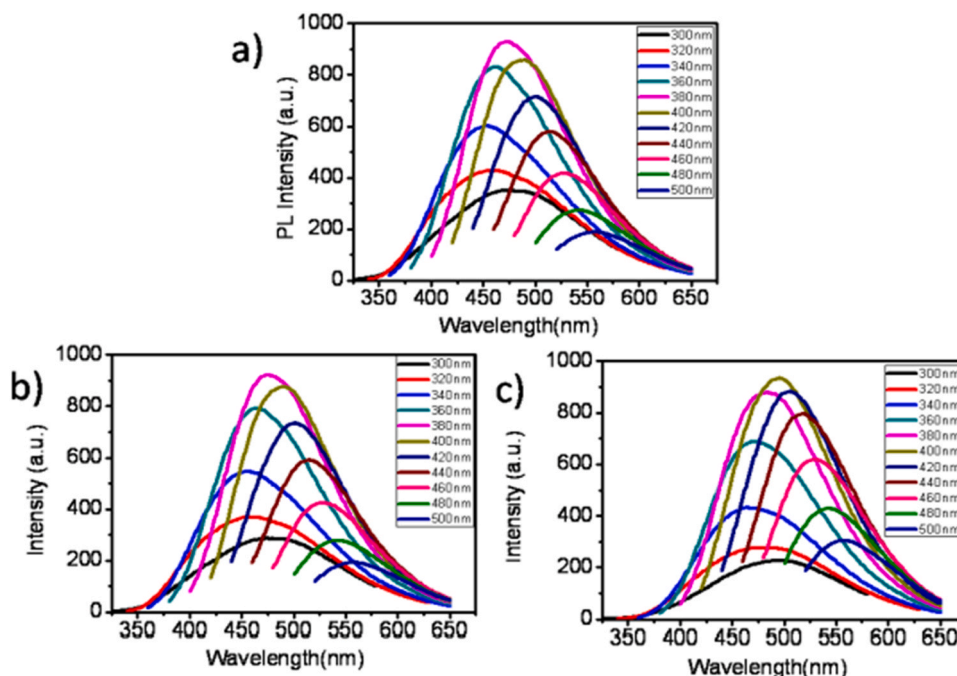


**Fig. 6.** PL spectra of the CDs obtained from glucose and formamide with different reaction time of 1 min (a), 2 min (b) and 5 min (c) at concentration of 0.25 mg/mL. Reprinted with permission from Ref. [30].

Despite others, the different type of reactor represents a key issue which makes the results from various investigations not properly comparable. In this context, further dedicated studies on the influence of the different parameters on the characteristics of the materials should be performed.

### CF applications of CDs

Three main strategies have been adopted to develop a CDs-based catalytic system operating under CF: i) to solubilize CDs in the feed solution to be delivered through a reactor (Fig. 8a) [50] ii) to support CDs in an inert and/or co-active bed which makes the catalytic system more easily recyclable (Fig. 8b) [51,52], and iii) to use a continuous and phase-transfer reactor in which CDs are used as the catalyst (Fig. 8c) [53]. The advantages and disadvantages of each one of those strategies will be discussed in the conclusions and future perspectives section.

### CDs solubilization in the feed solution

As far as strategy i) is concerned, Campalani et al. implemented a CD-photocatalyzed CF degradation of azo dyes, which are known as common hazardous contaminants (Fig. 8a) [50]. They first synthesized CDs in large amounts from fish waste (bass scales) through hydrothermal treatment (24 h, 200 °C) and then employed them as photocatalysts. It was found that CDs alone were less effective than when they were used in combination with an oxygen flow. Under the optimized conditions, by continuously delivering (flow = 0.5 mL/min) a solution of bass scales-derived CDs and the contaminant of choice (2 mg/mL and 5 ppm, respectively) in water together with an oxygen flow (0.78 mL/min) they demonstrated the procedure feasible for the degradation of methyl orange, acid red 18, amaranth, sunset yellow and chromotrope within 2 min under UV irradiation ( $\lambda = 365$  nm) at room temperature [50]. To the best of our knowledge, no other works on the use of such method have been reported so far.

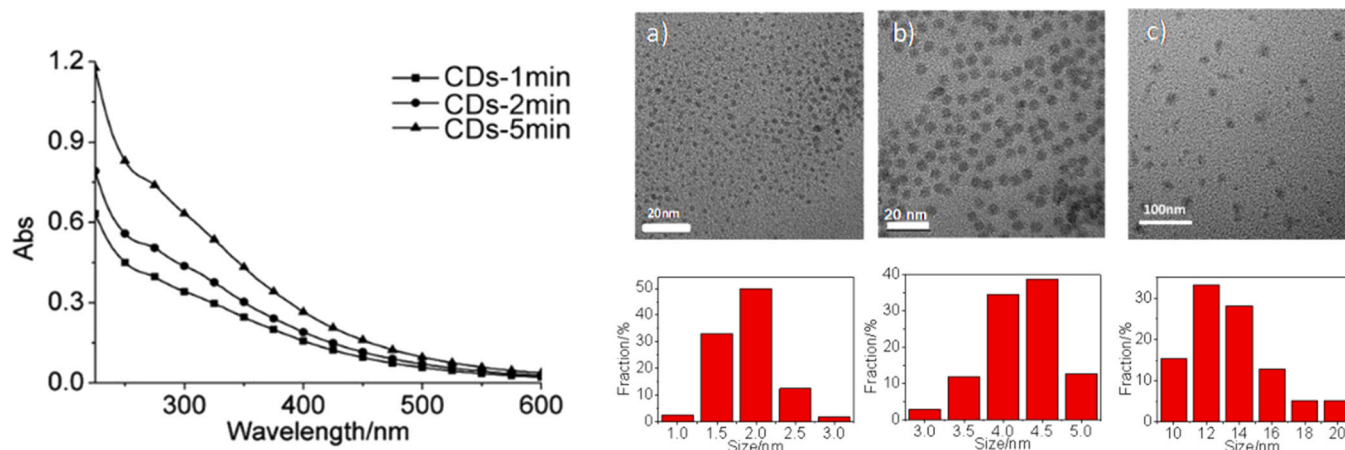


**Fig. 7.** UV-Vis spectra (left) and TEM images and size distribution (right) of CDs obtained by carbonization of glucose for 1 min (a), 2 min (b) and 5 min (c). Reprinted with permission from Ref. [30].

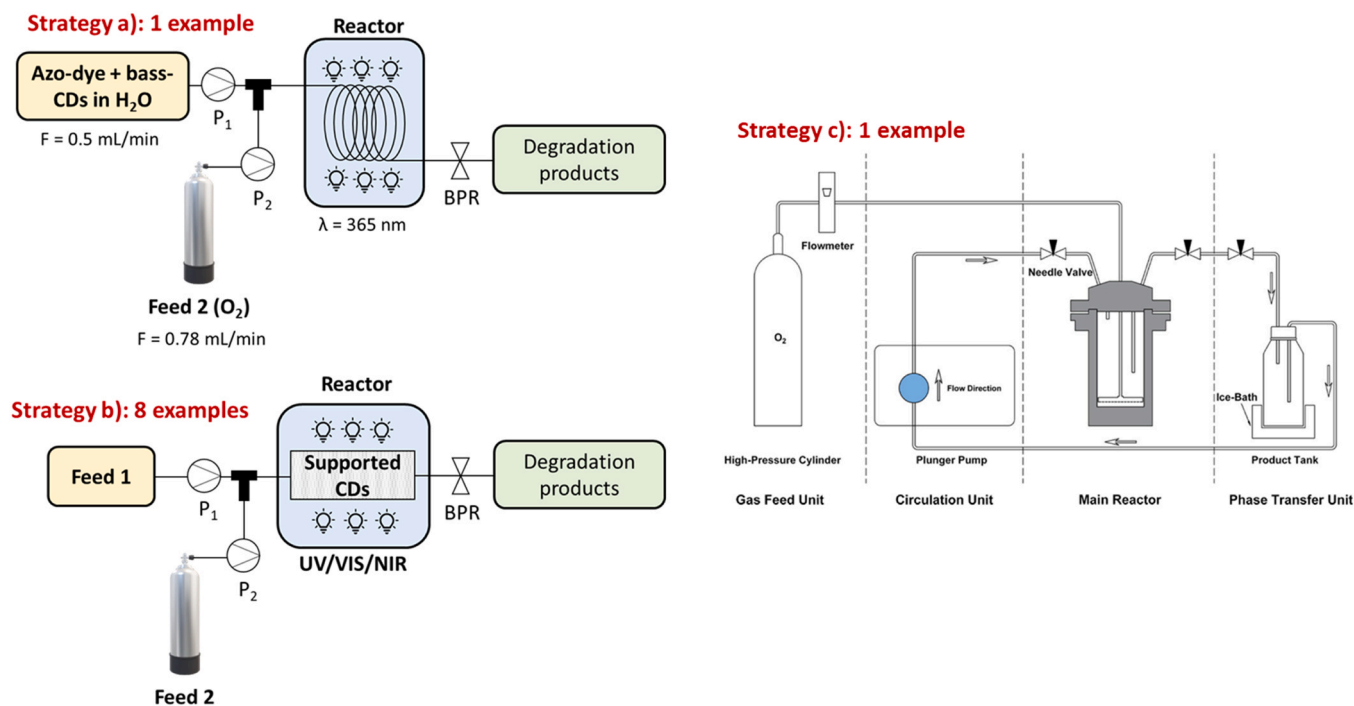


**Fig. 8.** Strategies for the CF application of CDs. a) CDs solubilization in the feed solution; b) Supported CDs methodologies; c) Continuous and phase-transfer reactor (Reprinted with permission from Ref. [53]. Copyright 2023, American Chemical Society.

### Supported CDs methodologies

The advantages of supporting CDs to create a recyclable catalyst have been exploited in different ways (Table 2). Tu et al. first synthesized carbon dots (CDs) from citric acid and urea in water using microwave-assisted methods (750 W,  $t = 5$  min) and then they immobilized them on  $\text{TiO}_2$  through ultrasonication for 30 min. Such CDs/ $\text{TiO}_2$  were employed for the CF degradation of acetone under UVA irradiation at room temperature (Table 2, entry 1) [52], reporting an acetone removal efficiency from water solution of  $0.21 \text{ mmol g}^{-1} \text{ h}^{-1}$  under non-optimized conditions ( $C_{\text{acetone}} = 254 \text{ ppm}$ ,  $C_{\text{water}} = 18.2 \text{ mg/L}$ , flow = 3 L/h). They reported that the CDs/ $\text{TiO}_2$  catalyst showed an improved performance for acetone removal than  $\text{TiO}_2$  alone, but the authors did not investigate the role of CDs in detail. In addition, CDs/ $\text{TiO}_2$  exhibited long-lasting performance under different water concentrations which is usually a significant parameter which impacts the performance of photocatalysts in general [52]. Das et al. synthesized C-dots from green herbs, and dill leaves following a single-step hydrothermal method ( $T = 180^\circ\text{C}$ ,  $t = 10$  h). The dots were first used as initiators for the photo-polymerization of poly(norepinephrine) under batch conditions (PNE; 6 examples) [51]. This CDs-promoted and UV-triggered polymerization was exploited for the fabrication of sandwich-like composite catalyst MXene/poly(norepinephrine)/copper nanoparticles (CDs/MPCN). In turn, the CDs/MPCN catalyst was supported on a cellulose filter paper, which was employed in the reduction of 4-nitrophenol (4-NP) to 4-aminophenol (4-AP) at ambient temperature (Table 2, entry 2 and Fig. 9) [51]. They achieved a maximized conversion of 4-NP (96%) at the flow rate of  $260.4 \text{ mL m}^{-2} \text{ h}^{-1}$ , while a further increase of the flow rate was detrimental for the reaction outcome. Even though the role of CDs for the reduction of 4-NP was not investigated and discussed in the paper, one cannot exclude a positive effect of CDs for the reaction.

Lin et al. synthesized  $\text{ZnO}_{1-x}$ /carbon dots composite hollow spheres via a single-step aerosol methodology, namely furnace aerosol reactor (FuAR) process reported elsewhere (4 examples) [59]. Those  $\text{ZnO}_{1-x}$ /CDs hollow composites showed great potential for the CF photocatalytic  $\text{CO}_2$  reduction over a broad UV-vis-NIR spectrum with  $\lambda$  in the range

250–950 nm at ambient temperature and pressure (Table 2, entry 3) [54]. At a  $\text{CO}_2$  flow rate of  $3 \text{ mL/min}$ , the best performing sample gave an average CO production rate of  $60.77 \mu\text{mol g}^{-1} \text{ h}^{-1}$ . This is about 54.7 times higher than that of pristine  $\text{ZnO}$ , and 11.5 times higher than that of commercial  $\text{TiO}_2$  (Degussa-P25), which are usually considered as benchmark catalysts in  $\text{CO}_2$  photoreduction [54]. A few years later, they also demonstrated that the  $\text{CO}_2$  photoreduction was excellently promoted by an oxygen-deficient  $\text{ZnO}$ /carbon dot (OD- $\text{ZnO}/\text{C}$ ) hybrid catalyst (6 examples), showing full spectrum (UV, visible and NIR light)-driven activity at room temperature (Table 2, entry 4) [55]. The built-up a gas flow reactor able to continuously deliver a mixture of  $\text{CO}_2/\text{H}_2\text{O}$  vapour (flow rate =  $3 \text{ mL/min}$ ), obtained by passing  $\text{CO}_2$  through a water bubbler, into a CDs-activated photocatalyst reactor in different wavelength regions ( $\lambda = 250\text{--}950 \text{ nm}$ ,  $400\text{--}950 \text{ nm}$ , and  $715\text{--}950 \text{ nm}$ ) [55]. For the best performing catalyst, quantum yields of 0.26%, 0.13% and 0.05% under UV-Vis-NIR, Vis-NIR and NIR light, respectively, in the production of CO were found. Intriguingly, they proved that defects present in the catalyst increased the light utilization efficiency within the UV-Vis to NIR region, while ensuring an efficient adsorption and activation of the  $\text{CO}_2/\text{H}_2\text{O}$  vapor.

Hu et al. employed CDs to enhance the photocatalytic performance of  $\text{TiO}_2$ -based composites for the removal of acetaldehyde under CF (Table 2, entry 5) [56]. The authors synthesized CDs from citric acid and urea (1:1 wt/wt) through hydrothermal treatment ( $T = 180^\circ\text{C}$ ,  $t = 6$  h) and then immobilize them on  $\text{TiO}_2$  by dispersion in  $\text{H}_2\text{O}/\text{EtOH}$  mixture followed by calcination of the residual solids at  $300^\circ\text{C}$ . The removal of a continuous flow of gaseous acetaldehyde (500 ppm,  $20 \text{ mL/min}$ ) was performed with 99% efficiency under fluorescent lamp irradiation ( $\lambda > 380 \text{ nm}$ ). This was more than 2 times higher than when pristine  $\text{TiO}_2$  was employed [56]. Qu et al. synthesized N,S-doped carbon quantum dot (N,S-CQD) via hydrothermal treatment ( $T = 180^\circ\text{C}$ ,  $t = 10$  h) starting from L-cysteine, ethylene glycol and nitric acid. Then, they synthesized a  $\text{ZnO}/\text{N,S-CQDs}$  hybrid nanoflower via one-pot hydrothermal process ( $T = 100^\circ\text{C}$ ,  $t = 12$  h) [57]. The synthesized CDs-based catalyst showed photocatalytic activity under sunlight irradiation for the degradation of antibiotics and other pollutants, such as ciprofloxacin (CIP) cephalixin (CEL), methylene blue



**Table 2**  
Strategies for the immobilization of CDs in different applications.

Entry	Support	Application	Ref.
1	TiO <sub>2</sub>	Degradation of acetone under UV irradiation	[52]
2	Cellulose	Reduction of 4-nitrophenol	[51]
3	ZnO <sub>1-x</sub>	CO <sub>2</sub> photoreduction over UV-vis-NIR spectrum	[54]
4	Oxygen-deficient ZnO	CO <sub>2</sub> photoreduction over UV-vis-NIR spectrum	[55]
5	TiO <sub>2</sub> -based composites	Acetaldehyde removal	[56]
6	ZnO and NH <sub>2</sub> -decorated quartz	Degradation of antibiotics and pollutants	[57]
7	Mesoporous silicon nanoparticles	Ultrasensitive detection of aflatoxin B1 and Staphylococcus aureus	[58]

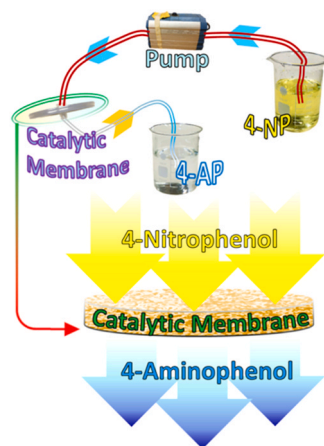


**Fig. 9.** CF conversion of 4-nitrophenol into 4-aminophenol following the protocol reported by Das et al.

Adapted with permission from Ref. [51]. Copyright 2023 American Chemical Society.

(MB), rhodamine B (RhB) or malachite green (MG) (Table 2, entry 6). Intriguingly, they further supported the ZnO/N,S-CQDs into quartz capillary tubes to employ them in the CF mode. The methodology consisted in functionalizing with -NH<sub>2</sub> groups the inner walls of quartz capillary tubes using 3-aminopropyltriethoxysilane (APTES) and, simultaneously, connecting to the modified tubes with the ZnO/N,S-CQDs via hydrogen bonding (Fig. 10) [57]. By using the functionalized quartz capillary tubes as photoreactors, they obtained a 42.1% degradation efficiency of CIP under the best conditions ( $t = 90$  min; flow rate = 2 mL/min) [57].

Wang et al. first prepared silanized CDs (SiL-CDS) by an hydrothermal method ( $T = 160$  °C,  $t = 4$  h) from rose bengal sodium salt and N-[3-(Trimethoxysilyl)propyl]ethylenediamine. Then, they developed a procedure to covalently bound SiL-CDS with mesoporous silicon nanoparticles to be used to build up lateral flow immunoassays (LFIAs) for the ultrasensitive detection of aflatoxin B1 (AFB1) and Staphylococcus aureus (*S. aureus*) (Table 2, entry 7). They were able to achieve quantitative detection limits of 0.05 ng/mL and 10<sup>2</sup> cfu/mL for AFB1 and *S. aureus*, respectively [58].

Noteworthy, one report on the use of CDs as support in the preparation of photoactive catalysts is present in the literature, too. Hence, starting from alkali lignin and ethylenediamine, Zhuang and co-workers obtained N-doped lignin-based carbon dots (LCDs) according to a hydrothermal method ( $T = 190$  °C,  $t = 12$  h), which were used as the support for Pt single atoms [60]. The complete procedure for the synthesis of the catalyst is reported in Fig. 11. The first step consists in the Pt-anchoring on the LCDs by a liquid-phase photoreduction method. The resulting Pt-LCDs were, then, deposited on CdS nano rods via ultrasound assisted mixing to obtain the final catalyst (Pt-LCDs@CdS). Such catalyst was found active for 60 h in the visible-light-promoted photocatalytic H<sub>2</sub>-evolution, reaching a rate up to 46.10 mmol h<sup>-1</sup> g<sup>-1</sup>. Even though the methodology was not formally developed under

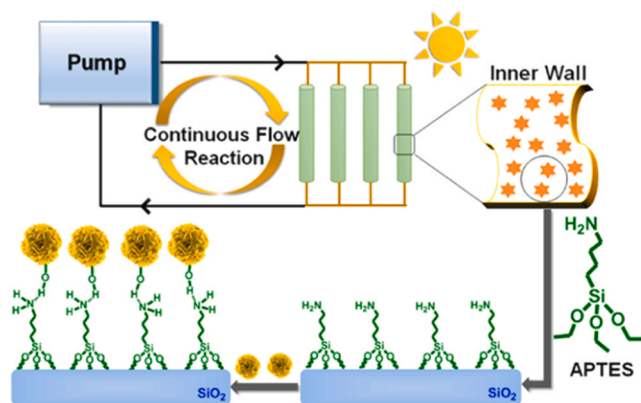


**Fig. 10.** Methodology for the immobilization of ZnO/N,S-CQDs onto quartz capillary tubes.

Reprinted with permission from Ref. [57].

continuous flow, the long photostability of the catalyst and the possibility of continuously producing H<sub>2</sub> makes this work worth of note in the present review.

#### Continuous and phase-transfer reactor

One example on the implementation of a continuous and phase transfer reactor was reported in the literature. In detail, a machine learning (mL)-guided protocol for the fabrication of metal-free carbon dot active as homogeneous catalysts for C-H bond oxidation was developed [53]. CDs were synthesized from ascorbic acid following a microwave-assisted mechanochemical method consisting of simultaneously heating (800 W,  $t = 0.5$  h) and grinding the ascorbic acid powder. Such dots showed good activity towards the oxidation of cyclohexane to adipic acid in the presence of O<sub>2</sub> ( $p = 5$ –50 bar) both in batch and under CF conditions ( $T = 90$ –180 °C,  $t = 2$ –24 h). To perform the reaction under CF, the authors designed a continuous and phase transfer reactor (Fig. 8c), where CDs were used as the catalysts. Inside the reactor an O<sub>2</sub> gas feed was dispersed into microbubbles together with cyclohexane which continuously produced a liquid mixture of cyclohexane and adipic acid (AA). In turn, AA crystals were precipitated in the product tank. At the same time, the liquid in the product tank was pumped back and fresh cyclohexane was continuously added into the main reactor from another feed inlet, affording the continuous oxidation of cyclohexane into AA [53]. Under the best achieved conditions ( $T = 150$  °C,  $p = 20$  bar,  $t = 4$  h), the authors reached a 16.32% yield per hour of AA.

#### Other in-continuous applications of CDs

The most spread CF utilization of CDs is, to date, their use as photocatalysts. Nevertheless, a short section which includes some examples on the use of CDs in-continuous represents an interesting topic to be included in the present review. More detailed overviews on the application of CDs in different fields have been recently reviewed elsewhere [61–64].



**Fig. 11.** Overall process for the fabrication of Pt-NLCDs@CdS reported by Zhuang et al. Reprinted with permission from Ref. [60].

N-, S-doped CDs found an interesting field of application in bio-imaging of human endothelial cells both under confocal and flow conditions [65]. Zhong et al. synthesized CDs from *m*-phenylenediamine and tobias acid through a hydrothermal method ( $T = 200\text{ }^{\circ}\text{C}$ ,  $t = 10\text{ h}$ ) obtaining N-, S-doped CDs with a quantum yield up to 37.2%. Such CDs showed low cytotoxicity, low hemolysis rate ( $< 0.5\%$ ) and were able to

keep their activity even in the presence of different inhibitors (Fig. 12). The authors claimed that after 3 h incubation the N-, S-CDs are able to penetrate the lipid bilayer of the cell membrane into the cytoplasm, which makes them suitable for bio-imaging thanks to their fluorescence. Similarly, Chen et al. found a similar application for their N-,S-doped CDs together with the continuous detection of Cr<sub>2</sub>O<sub>7</sub><sup>2-</sup> ions [66].

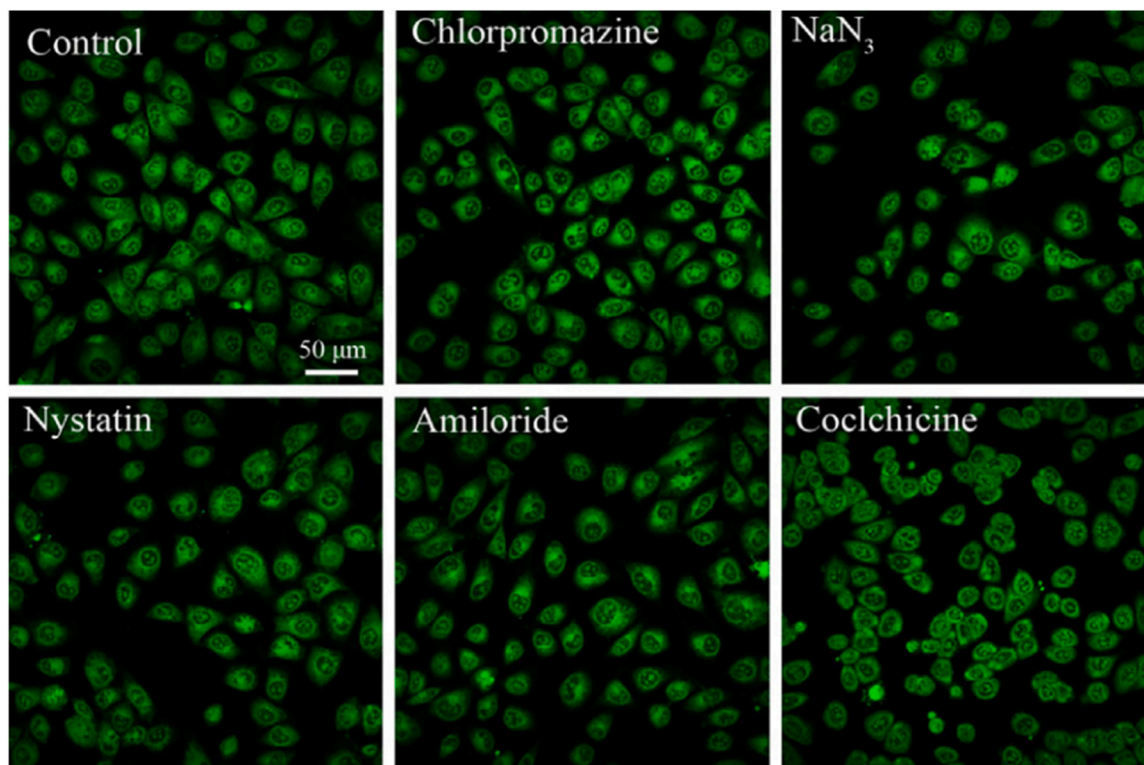


**Fig. 12.** Confocal images of HUVEC cells incubated with N, S-CDs for 3 h and pretreated with different inhibitors. Reproduced with permission from Ref. [65].

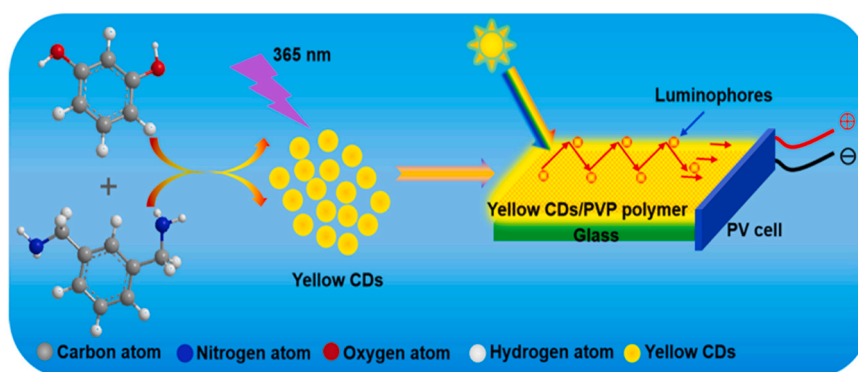


Fig. 13. Gong et al. methodology for the fabrication of luminescent solar concentrators (LSCs). Reprinted with permission from Ref. [68].

Worth noting is the use of CDs for the continuous energy production/storage. In that regard, Gong et al. applied silicon-doped carbon dots (Si-CDs) for energy storage in luminescent solar concentrators (LSCs) [67]. The synthesized Si-CDs showed an excellent quantum yield of 92.3%. The dots were prepared by reacting rhodamine B (20 mg) with Na-metasilicate (0.5 g) in deionized water ( $T = 180\text{ }^{\circ}\text{C}$ ,  $t = 12\text{ h}$ ). LSCs were fabricated by a drop coating method: a Si-CDs/polyvinylpyrrolidone solution in MeOH was casted at room temperature on a glass surface to obtain a thin layer of Si-CDs in different concentrations (6 examples). The best performing sample with a 0.2% concentration of Si-CDs allowed to reach a 4.36% power conversion efficiency (PCE) in a film structured LSC ( $5 \times 5 \times 0.2\text{ cm}^3$ ). When the surface of LSC was increased to  $15 \times 15\text{ cm}^3$  a lower value for PCE (2.06%) was obtained. A similar approach (Fig. 13) has been recently used by the same group using yellow emitting CDs which allowed to improve the PCE up to 4.1% under natural sunlight with a  $10 \times 10\text{ cm}^2$  LSC [68].

## Conclusions and future perspectives

Herein we summarized the reported protocols for CF synthesis and applications of CDs. To conclude this mini-review, our perspective on the possible future trends and challenges in the field is given.

Along with all the up-cited potential advantages of CF synthesis of CDs, few limitations, generally of a technological nature, need to be addressed: in particular, major challenges still remain the scale up and the control of the nano-particles size and properties. This hampers their widespread use and hinders their potential for certain (*i.e.* photocatalytic) applications. The development of lab scale CF microfluidic reactors able to convert various renewable C-/N-/S-sources (among others) into CDs is the first step towards a future implementation of such methodologies at an industrial level. Effort should be made to design reaction systems able to endlessly operate, at least theoretically, and able to avoid clogging of the nanodots inside the reactor. The risk of precipitation resulting in channel clogging is, indeed, one of the most common problems encountered in micro fluidic synthesis, requiring careful design of reactor and conditions. Even though clogging seems a simple problem to overcome, usually it is the major challenge for the scale up of CF systems and reactors, especially when microfluidic is concerned. In that regard, our vision to overcome such issues is twofold. i) Engineering proper CF reactors for instance by fabricating them with inert materials in the inner surface which minimize the interactions between the nanodots and the reactor itself. In addition, the reactor's dimension and shape are other critical aspects to be considered to avoid/minimize clogging. ii) By the fine choice of suitable solvents able to fully solubilize both the starting material and CDs after their synthesis. In that regard, water is of course the first choice both from an environmental standpoint and since it allows to conduct the reactions under supercritical conditions, but it is not the only one. Mixtures of

water with other polar solvents (*i.e.* ethanol) and ionic liquid/DES can be other suitable options. In addition, from this literature review it becomes clear that more effort should be made in investigating the effect of the processing conditions and the experimental (*i.e.* CF reactor) set up on the characteristics and properties of CDs.

Notwithstanding that the use of CDs as (photo-)catalyst in CF applications is still in its infancy, the pioneering investigations listed above represent a good starting point for future development. The solubilization of CDs in the feed solution seems the most straightforward strategy for their use in CF catalysis and other applications (*i.e.* analytical). This allows for an easy solubilization and consequently mass transfer from the reactants mixture to the dots. A drawback of such strategy is found in the separation of the nanoparticles from the products mixture and their recycling once the reaction is complete, which makes CDs a "single use" catalyst. The methodology becomes attractive especially only within the perspective of synthesizing CDs in large scale and by producing them from low cost (possible waste streams-derived) starting materials. On the other hand, to better valorize and recycle such valuable nano materials, the immobilization of CDs represents a valuable opportunity. While being interesting from the CDs recycle standpoint, this pathway hinders some issues related to the mass transfer of the reagents towards the active sites of CDs, depending not only on the dots behavior but also on the characteristics of the support. In addition, the use of CDs as photocatalysts in CF should be expanded to organic transformation reactions of wide interest: their use in combination with classical catalysts can pave the way towards new synthetic pathways for the obtainment of platform chemicals. The concatenation of different CF reactors to perform different synthetic steps involving CDs is still an underexplored topic. As highlighted in the previous paragraph, some examples are bio-continuous imaging and continuous energy production and storage. The continuous detection of pollutants, such as heavy metals ions, can be an interesting field of research that can expand the utilization of CDs using CF reactors. Other opportunities are found in electro catalysis and in multi-step organic synthesis.

Other open challenges are the standardization of synthetic and purification protocols. Particular attention should be paid to develop a standardized purification method since the variety of existing synthetic pathways can lead to the presence of molecular entities that can mimic the behavior of CDs and interfere or alter their photocatalytic activity. As already mentioned, a strict control over the structural aspects of CDs is also crucial. The great variety of functional groups that can be found on the surface of the carbonaceous nanoparticles, indeed, can heavily influence their properties. In this frame, however, the CF synthesis of the nanomaterials can help in having a more careful control over specific parameters leading to a more reproducible production of CDs.

Overall, CF technologies are a promising alternative to batch reactors for the synthesis of CDs and for their (photo-)catalytic application. It is hoped that efforts made to collect and analyze data,



information, interpretations and insights in this review may be beneficial to inspire researchers and scientists to develop novel CF systems able either to convert different renewable starting materials into CDs or to use CDs as catalysts in CF reactions.

### Declaration of Competing Interest

The authors declare the following financial interests/personal relationships which may be considered as potential competing interests: Davide Rigo reports was provided by Aalto University.

### Acknowledgements

Professor Maurizio Selva and Professor Alvise Perosa are kindly acknowledged for their mentoring. Fondazione Cariverona is gratefully acknowledged for funding the project “Valorizzazione di scarti agroalimentari per nuovi cosmetici green” ID no. 1174 – Cod. SIME no. 2019.0428.

### References

- [1] M.B. Plutschack, B. Pieber, K. Gilmore, P.H. Seeberger, The Hitchhiker’s guide to flow chemistry, *Chem. Rev.* 117 (2017) 11796–11893, <https://doi.org/10.1021/acs.chemrev.7b00183>
- [2] V.P. Bucci, Process intensification strategy, *Macromolecules* (2000) 22–34.
- [3] Z. Qiao, Z. Wang, C. Zhang, S. Yuan, Y. Zhu, J. Wang, S. Wang, PVAm-PIP/PS composite membrane with high performance for CO<sub>2</sub>/N<sub>2</sub> separation, *AIChE J.* 59 (2013) 215–228, <https://doi.org/10.1002/aic.13781>
- [4] R. Gérardy, N. Emmanuel, T. Toupay, V.E. Kassim, N.N. Tshibalonza, M. Schmitz, J.C.M. Monbaliu, Continuous flow organic chemistry: successes and pitfalls at the interface with current societal challenges, *Eur. J. Org. Chem.* (2018) 2301–2351, <https://doi.org/10.1002/ejoc.201800149>
- [5] J. Wegner, S. Ceylan, A. Kirschning, Flow chemistry – a key enabling technology for (multistep) organic synthesis, *Adv. Synth. Catal.* 354 (2012) 17–57, <https://doi.org/10.1002/adsc.201100584>
- [6] A. Tanimu, S. Jaenicke, K. Alhooshani, Heterogeneous catalysis in continuous flow microreactors: a review of methods and applications, *Chem. Eng. J.* 327 (2017) 792–821, <https://doi.org/10.1016/j.cej.2017.06.161>
- [7] B. Gutmann, D. Cantillo, C.O. Kappe, Continuous-flow technology – a tool for the safe manufacturing of active pharmaceutical ingredients, *Angew. Chem. Int. Ed.* 54 (2015) 6688–6728, <https://doi.org/10.1002/anie.201409318>
- [8] Y. Li, Y. Zhao, H. Cheng, Y. Hu, G. Shi, L. Dai, L. Qu, Nitrogen-doped graphene quantum dots with oxygen-rich functional groups, *J. Am. Chem. Soc.* 134 (2012) 15–18, <https://doi.org/10.1021/ja206030c>
- [9] Y. Dong, H. Pang, H. Bin Yang, C. Guo, J. Shao, Y. Chi, C.M. Li, T. Yu, Carbon-based dots co-doped with nitrogen and sulfur for high quantum yield and excitation-independent emission, *Angew. Chem. Int. Ed.* 52 (2013) 7800–7804, <https://doi.org/10.1002/anie.201301114>
- [10] X. Yang, X. Li, B. Wang, L. Ai, G. Li, B. Yang, S. Lu, Advances, opportunities, and challenge for full-color emissive carbon dots, *Chin. Chem. Lett.* 33 (2022) 613–625, <https://doi.org/10.1016/j.ccl.2021.08.077>
- [11] E. Amadio, S. Cailotto, C. Campalani, L. Branzi, C. Raviola, D. Ravelli, E. Cattaruzza, E. Trave, A. Benedetti, M. Selva, A. Perosa, Precursor-dependent photocatalytic activity of carbon dots, *Molecules* 25 (2019) 101, <https://doi.org/10.3390/molecules25010101>
- [12] S.N. Baker, G.A. Baker, Luminescent carbon nanodots: emergent nanolights, *Angew. Chem. Int. Ed.* 49 (2010) 6726–6744, <https://doi.org/10.1002/anie.200906623>
- [13] H. Li, Z. Kang, Y. Liu, S.T. Lee, Carbon nanodots: synthesis, properties and applications, *J. Mater. Chem.* 22 (2012) 24230–24253, <https://doi.org/10.1039/c2jm34690g>
- [14] S. Cailotto, E. Amadio, M. Facchin, M. Selva, E. Pontoglio, F. Rizzolio, P. Riello, G. Toffoli, A. Benedetti, A. Perosa, Carbon-dots from sugars and ascorbic acid: role of the precursors on morphology, properties, toxicity and drug uptake, *ACS Med. Chem. Lett.* 9 (2018) 832–837, <https://doi.org/10.1021/acsmchemlett.8b00240>
- [15] S.W. Huang, Y.F. Lin, Y.X. Li, C.C. Hu, T.C. Chiu, Synthesis of fluorescent carbon dots as selective and sensitive probes for cupric ions and cell imaging, *Molecules* 24 (2019) 1–12, <https://doi.org/10.3390/molecules24091785>
- [16] M. Tuerhong, Y. Xu, X.B. Yin, Review on carbon dots and their applications, *Chin. J. Anal. Chem.* 45 (2017) 139–150, [https://doi.org/10.1016/S1872-2040\(16\)60990-8](https://doi.org/10.1016/S1872-2040(16)60990-8)
- [17] C. Campalani, V. Causin, M. Selva, A. Perosa, Fish-waste-derived gelatin and carbon dots for biobased UV-blocking films, *ACS Appl. Mater. Interfaces* 14 (2022) 35148–35156, <https://doi.org/10.1021/acsmami.2c11749>
- [18] R. Fu, H. Song, X. Liu, Y. Zhang, G. Xiao, B. Zou, G.I.N. Waterhouse, S. Lu, Disulfide crosslinking-induced aggregation: towards solid-state fluorescent carbon dots with vastly different emission colors, *Chin. J. Chem.* 41 (2023) 1007–1014, <https://doi.org/10.1002/cjoc.202200736>
- [19] Y. Wu, J. Li, X. Zhao, X. Gong, Nickel-doped carbon dots with enhanced and tunable multicolor fluorescence emission for multicolor light-emitting diodes, *Carbon* 201 (2023) 796–804, <https://doi.org/10.1016/j.carbon.2022.09.060>
- [20] J. Li, X. Gong, The emerging development of multicolor carbon dots, *Small* 18 (2022) 2205099, <https://doi.org/10.1002/smll.202205099>
- [21] S. Cailotto, D. Massari, M. Gigli, C. Campalani, M. Bonini, S. You, A. Vomiero, M. Selva, A. Perosa, C. Crestini, N-doped carbon dot hydrogels from brewing waste for photocatalytic wastewater treatment, *ACS Omega* 7 (2022) 4052–4061, <https://doi.org/10.1021/acsomega.1c05403>
- [22] C. Campalani, E. Cattaruzza, S. Zorzi, A. Vomiero, S. You, L. Matthews, M. Capron, C. Mondelli, M. Selva, A. Perosa, Biobased carbon dots: from fish scales to photocatalysis, *Nanomaterials* 11 (2021) 524, <https://doi.org/10.3390/nano11020524>
- [23] C. Campalani, N. Bragato, A. Morandini, M. Selva, G. Fiorani, A. Perosa, Carbon dots as green photocatalysts for atom transfer radical polymerization of methacrylates, *Catal. Today* 418 (2023) 114039, <https://doi.org/10.1016/j.cattod.2023.114039>
- [24] D. Rigo, G. Fiorani, A. Perosa, M. Selva, Acid-catalyzed reactions of isopropenyl esters and renewable diols: a 100 % carbon efficient transesterification/acetallization tandem sequence, from batch to continuous flow, *ACS Sustain. Chem. Eng.* 7 (2019) 18810–18818, <https://doi.org/10.1021/acssuschemeng.9b03359>
- [25] D. Rigo, R. Calmanti, A. Perosa, M. Selva, G. Fiorani, Diethylene glycol/NaBr catalyzed CO<sub>2</sub> insertion into terminal epoxides: from batch to continuous flow, *ChemCatChem* 13 (2021) 2005–2016, <https://doi.org/10.1002/cctc.202002010>
- [26] D. Rigo, N.A. Carmo Dos Santos, A. Perosa, M. Selva, Concatenated batch and continuous flow procedures for the upgrading of glycerol-derived aminodiols via N-acetylation and acetalization reactions, *Catalysts* 11 (2021) 1–12, <https://doi.org/10.3390/catal11010021>
- [27] B. Bartolomei, J. Dosso, M. Prato, New trends in nonconventional carbon dot synthesis, *Trends Chem.* 3 (2021) 943–953, <https://doi.org/10.1016/j.trechm.2021.09.003>
- [28] A.G. Niculescu, C. Chircov, A.C. Bîrcă, A.M. Grumezescu, Nanomaterials synthesis through microfluidic methods: an updated overview, *Nanomaterials* 11 (2021), <https://doi.org/10.3390/nano11040864>
- [29] P. Bianchi, G. Petit, J.C.M. Monbaliu, Scalable and robust photochemical flow process towards small spherical gold nanoparticles, *React. Chem. Eng.* 5 (2020) 1224–1236, <https://doi.org/10.1039/d0re00092b>
- [30] Y. Lu, L. Zhang, H. Lin, The use of a microreactor for rapid screening of the reaction conditions and investigation of the photoluminescence mechanism of carbon dots, *Chem. Eur. J.* 20 (2014) 4246–4250, <https://doi.org/10.1002/chem.201304358>
- [31] Y. Cheng, Z. Chen, Y. Wang, J. Xu, Continuous synthesis of N, S co-doped carbon dots for selective detection of Cd (II) ions, *J. Photochem. Photobiol. A* 429 (2022) 113910, <https://doi.org/10.1016/j.jphotochem.2022.113910>
- [32] L. Rao, Y. Tang, Z. Li, X. Ding, G. Liang, H. Lu, C. Yan, K. Tang, B. Yu, Efficient synthesis of highly fluorescent carbon dots by microreactor method and their application in Fe<sup>3+</sup> ion detection, *Mater. Sci. Eng. C* 81 (2017) 213–223, <https://doi.org/10.1016/j.msec.2017.07.046>
- [33] M. Berenguel-Alonso, I. Ortiz-Gómez, B. Fernández, P. Couceiro, J. Alonso-Chamarro, L.F. Capitán-Vallvey, A. Salinas-Castillo, M. Puyol, An LTCC monolithic microreactor for the synthesis of carbon dots with photoluminescence imaging of the reaction progress, *Sens. Actuators B Chem.* 296 (2019) 126613, <https://doi.org/10.1016/j.snb.2019.05.090>
- [34] S.G. De Pedro, A. Salinas-Castillo, M. Ariza-Avidad, A. Lapresta-Fernández, C. Sánchez-González, C.S. Martínez-Cisneros, M. Puyol, L.F. Capitán-Vallvey, J. Alonso-Chamarro, Microsystem-assisted synthesis of carbon dots with fluorescent and colorimetric properties for pH detection, *Nanoscale* 6 (2014) 6018–6024, <https://doi.org/10.1039/c4nr00573b>
- [35] A. Hebbur, R. Selvaraj, R. Vinayagam, T. Varadavenkatesan, P.S. Kumar, P.A. Duc, G. Rangasamy, A critical review on the environmental applications of carbon dots, *Chemosphere* 313 (2023) 137308, <https://doi.org/10.1016/j.chemosphere.2022.137308>
- [36] L. Rao, Y. Tang, H. Lu, S. Yu, X. Ding, K. Xu, Z. Li, J.Z. Zhang, Highly photoluminescent and stable n-doped carbon dots as nanoprobe for Hg<sup>2+</sup> detection, *Nanomaterials* 8 (2018) 1–18, <https://doi.org/10.3390/nano8110900>
- [37] Y. Tang, L. Rao, Z. Li, H. Lu, C. Yan, S. Yu, X. Ding, B. Yu, Rapid synthesis of highly photoluminescent nitrogen-doped carbon quantum dots via a microreactor with foamy copper for the detection of Hg<sup>2+</sup> ions, *Sens. Actuators B Chem.* 258 (2018) 637–647, <https://doi.org/10.1016/j.snb.2017.11.140>
- [38] I.A. Baragau, Z. Lu, N.P. Power, D.J. Morgan, J. Bowen, P. Diaz, S. Kellici, Continuous hydrothermal flow synthesis of S-functionalised carbon quantum dots for enhanced oil recovery, *J. Chem. Eng.* 405 (2021) 126631, <https://doi.org/10.1016/j.cej.2020.126631>
- [39] I.A. Baragau, N.P. Power, D.J. Morgan, T. Heil, R.A. Lobo, C.S. Roberts, M.M. Titirici, S. Dunn, S. Kellici, Continuous hydrothermal flow synthesis of blue-luminescent, excitation-independent nitrogen-doped carbon quantum dots as nanosensors, *J. Mater. Chem. A* 8 (2020) 3270–3279, <https://doi.org/10.1039/c9ta11781d>
- [40] I.A. Baragau, N.P. Power, D.J. Morgan, R.A. Lobo, C.S. Roberts, M.M. Titirici, V. Middelkoop, A. Diaz, S. Dunn, S. Kellici, Efficient continuous hydrothermal flow synthesis of carbon quantum dots from a targeted biomass precursor for on-off metal ions nanosensing, *ACS Sustain. Chem. Eng.* 9 (2021) 2559–2569, <https://doi.org/10.1021/acssuschemeng.0c08594>
- [41] S. Kellici, J. Acord, K.E. Moore, N.P. Power, V. Middelkoop, D.J. Morgan, T. Heil, P. Coppo, I.A. Baragau, C.L. Raston, Continuous hydrothermal flow synthesis of graphene quantum dots, *React. Chem. Eng.* 3 (2018) 949–958, <https://doi.org/10.1039/c8re00158h>
- [42] S. Kellici, J. Acord, N.P. Power, D.J. Morgan, P. Coppo, T. Heil, B. Saha, Rapid synthesis of graphene quantum dots using a continuous hydrothermal flow synthesis approach, *RSC Adv.* 7 (2017) 14716–14720, <https://doi.org/10.1039/c7ra00127d>
- [43] K.G. Nguyen, I.A. Baragau, R. Gromicova, A. Nicolaev, S.A.J. Thomson, A. Rennie, N.P. Power, M.T. Sajjad, S. Kellici, Investigating the effect of N-doping on carbon



- quantum dots structure, optical properties and metal ion screening, *Sci. Rep.* 12 (2022) 1–12, <https://doi.org/10.1038/s41598-022-16893-x>
- [44] M. Shao, Q. Yu, N. Jing, Y. Cheng, D. Wang, Y.D. Wang, J.H. Xu, Continuous synthesis of carbon dots with full spectrum fluorescence and the mechanism of their multiple color emission, *Lab Chip* 19 (2019) 3974–3978, <https://doi.org/10.1039/c9lc00683d>
- [45] C. Fu, L. Qiang, T. Liu, L. Tan, H. Shi, X. Chen, X. Ren, X. Meng, Ultrafast chemical aerosol flow synthesis of biocompatible fluorescent carbon dots for bioimaging, *J. Mater. Chem. B* 2 (2014) 6978–6983, <https://doi.org/10.1039/c4tb01004c>
- [46] S. Guo, J. Lan, B. Liu, B. Zheng, X. Gong, X. Fan, Continuous flow synthesis of N-doped carbon quantum dots for total phenol content detection, *Chemosensors* 10 (2022) 1–16, <https://doi.org/10.3390/chemosensors10080334>
- [47] L. Lin, Y. Yin, Z. Li, H. Xu, V. Hessel, K.K. Ostrikov, Continuous microflow synthesis of fluorescent phosphorus and nitrogen co-doped carbon quantum dots, *Chem. Eng. Res. Des.* 178 (2022) 395–404, <https://doi.org/10.1016/j.cherd.2021.12.037>
- [48] L. Lin, Y. Xia, H. Wen, W. Lu, Z. Li, H. Xu, J. Zhou, Green and continuous microflow synthesis of fluorescent carbon quantum dots for bio-imaging application, *AIChE J.* (2022) e17901, <https://doi.org/10.1002/aic.17901>
- [49] Y. Zhang, Y. Wang, X. Feng, F. Zhang, Y. Yang, X. Liu, Effect of reaction temperature on structure and fluorescence properties of nitrogen-doped carbon dots, *Appl. Surf. Sci.* 387 (2016) 1236–1246, <https://doi.org/10.1016/j.apsusc.2016.07.048>
- [50] C. Campalani, G. Petit, J.C.M. Monbaliu, M. Selva, A. Perosa, Continuous flow photooxidative degradation of azo dyes with biomass-derived carbon dots, *ChemPhotoChem* (2022) e202200234, <https://doi.org/10.1002/cptc.202200234>
- [51] P. Das, S. Ganguly, A. Saha, M. Noked, S. Margel, A. Gedanken, Carbon-dots-initiated photopolymerization: an in situ synthetic approach for MXene/poly(norepinephrine)/copper hybrid and its application for mitigating water pollution, *ACS Appl. Mater. Interfaces* 13 (2021) 31038–31050, <https://doi.org/10.1021/acsami.1c08111>
- [52] L.N.Q. Tu, L.T.K. Ngan, N.V.H. Nhan, N.Q. Long, Photodegradation of acetone vapor by carbon dots decorated TiO<sub>2</sub> catalyst: effects of experimental conditions, *IOP Conf. Ser.: Earth Environ. Sci.* 947 (2021) 012014, <https://doi.org/10.1088/1755-1315/947/1/012014>
- [53] X. Wang, S. Chen, Y. Ma, T. Zhang, Y. Zhao, T. He, H. Huang, S. Zhang, J. Rong, C. Shi, K. Tang, Y. Liu, Z. Kang, Continuous homogeneous catalytic oxidation of C–H bonds by metal-free carbon dots with a poly(ascorbic acid) structure, *ACS Appl. Mater. Interfaces* 14 (2022) 26682–26689, <https://doi.org/10.1021/acsami.2c03627>
- [54] L.Y. Lin, S. Kavadiya, B.B. Karakocak, Y. Nie, R. Raliya, S.T. Wang, M.Y. Berezin, P. Biswas, ZnO<sub>1-x</sub>/carbon dots composite hollow spheres: facile aerosol synthesis and superior CO<sub>2</sub> photoreduction under UV, visible and near-infrared irradiation, *Appl. Catal. B* 230 (2018) 36–48, <https://doi.org/10.1016/j.apcatb.2018.02.018>
- [55] L.Y. Lin, C. Liu, T.T. Hsieh, Efficient visible and NIR light-driven photocatalytic CO<sub>2</sub> reduction over defect-engineered ZnO/carbon dot hybrid and mechanistic insights, *J. Catal.* 391 (2020) 298–311, <https://doi.org/10.1016/j.jcat.2020.08.036>
- [56] Y. Hu, X. Xie, X. Wang, Y. Wang, Y. Zeng, D.Y.H. Pui, J. Sun, Visible-light upconversion carbon quantum dots decorated TiO<sub>2</sub> for the photodegradation of flowing gaseous acetaldehyde, *Appl. Surf. Sci.* 440 (2018) 266–274, <https://doi.org/10.1016/j.apsusc.2018.01.104>
- [57] Y. Qu, X. Xu, R. Huang, W. Qi, R. Su, Z. He, Enhanced photocatalytic degradation of antibiotics in water over functionalized N,S-doped carbon quantum dots embedded ZnO nanoflowers under sunlight irradiation, *J. Chem. Eng.* 382 (2020) 123016, <https://doi.org/10.1016/j.cjce.2019.123016>
- [58] Y. Wang, C. Deng, S. Qian, H. Li, P. Fu, H. Zhou, J. Zheng, An ultrasensitive lateral flow immunoassay platform for foodborne biotoxins and pathogenic bacteria based on carbon-dots embedded mesoporous silicon nanoparticles fluorescent reporter probes, *Food Chem.* 399 (2023), <https://doi.org/10.1016/j.foodchem.2022.133970>
- [59] G. Jian, L. Liu, M.R. Zachariah, Facile aerosol route to hollow CuO spheres and its superior performance as an oxidizer in nanoenergetic gas generators, *Adv. Funct. Mater.* 23 (2013) 1341–1346, <https://doi.org/10.1002/adfm.201202100>
- [60] J. Zhuang, S. Ren, B. Zhu, C. Han, Y.Y. Li, X. Zhang, H. Gao, M. Fan, Q. Tian, Lignin-based carbon dots as high-performance support of Pt single atoms for photocatalytic H<sub>2</sub> evolution, *J. Chem. Eng.* 446 (2022), <https://doi.org/10.1016/j.cjce.2022.136873>
- [61] C. Ji, Y. Zhou, R.M. Leblanc, Z. Peng, Recent developments of carbon dots in biosensing: a review, *ACS Sens* 5 (2020) 2724–2741, <https://doi.org/10.1021/acssensors.0c01556>
- [62] X. Sun, Y. Lei, Fluorescent carbon dots and their sensing applications, *Trends Anal. Chem.* 89 (2017) 163–180, <https://doi.org/10.1016/j.trac.2017.02.001>
- [63] M.L. Liu, B. Bin Chen, C.M. Li, C.Z. Huang, Carbon dots: synthesis, formation mechanism, fluorescence origin and sensing applications, *Green Chem.* 21 (2019) 449–471, <https://doi.org/10.1039/c8gc02736f>
- [64] D. Xu, Q. Lin, H.T. Chang, Recent advances and sensing applications of carbon dots, *Small Methods* 4 (2020), <https://doi.org/10.1002/smt.201900387>
- [65] J. Zhong, X. Chen, M. Zhang, C. Xiao, L. Cai, W.A. Khan, K. Yu, J. Cui, L. He, Blood compatible heteroatom-doped carbon dots for bio-imaging of human umbilical vein endothelial cells, *Chin. Chem. Lett.* 31 (2020) 769–773, <https://doi.org/10.1016/j.ccl.2020.01.007>
- [66] J. Chen, J. Liu, J. Li, L. Xu, Y. Qiao, One-pot synthesis of nitrogen and sulfur co-doped carbon dots and its application for sensor and multicolor cellular imaging, *J. Colloid Interface Sci.* 485 (2017) 167–174, <https://doi.org/10.1016/j.jcis.2016.09.040>
- [67] X. Gong, S. Zheng, X. Zhao, A. Vomiero, Engineering high-emissive silicon-doped carbon nanodots towards efficient large-area luminescent solar concentrators, *Nano Energy* 101 (2022) 107617, <https://doi.org/10.1016/j.nanoen.2022.107617>
- [68] J. Li, H. Zhao, X. Zhao, X. Gong, Boosting efficiency of luminescent solar concentrators using ultra-bright carbon dots with large Stokes shift, *Nanoscale Horiz.* 8 (2022) 83–94, <https://doi.org/10.1039/d2nh00360k>